NanoImpact 20 (2020) 100274

Contents lists available at ScienceDirect

NanoImpact

journal homepage: www.elsevier.com/locate/nanoimpact

Toxicogenomics analysis of dynamic dose-response in macrophages highlights molecular alterations relevant for multi-walled carbon nanotube-induced lung fibrosis

Laura A. Saarimäki [a,b,1], Pia A.S. Kinaret [c,1], Giovanni Scala [d], Giusy del Giudice [a,b], Antonio Federico [a,b], Angela Serra [a,b], Dario Greco [a,b,c,*]

[a] Faculty of Medicine and Health Technology, Tampere University, 33520 Tampere, Finland
[b] BioMediTech Institute, Tampere University, 33520 Tampere, Finland
[c] Institute of Biotechnology, Helsinki Institute of Life Science, University of Helsinki, 00790 Helsinki, Finland
[d] Department of Biology, University of Naples Federico II, 80126 Naples, Italy

ARTICLE INFO

Keywords:
Multi-omics
Multi-walled carbon nanotubes
Mechanism of action
Toxicogenomics

ABSTRACT

Toxicogenomics approaches are increasingly used to gain mechanistic insight into the toxicity of engineered nanomaterials (ENMs). These emerging technologies have been shown to aid the translation of *in vitro* experimentation into relevant information on real-life exposures. Furthermore, integrating multiple layers of molecular alteration can provide a broader understanding of the toxicological insult. While there is growing evidence of the immunotoxic effects of several ENMs, the mechanisms are less characterized, and the dynamics of the molecular adaptation of the immune cells are still largely unknown.

Here, we hypothesized that a multi-omics investigation of dynamic dose-dependent (DDD) molecular alterations could be used to retrieve relevant information concerning possible long-term consequences of the exposure. To this end, we applied this approach on a model of human macrophages to investigate the effects of rigid multi-walled carbon nanotubes (rCNTs). THP-1 macrophages were exposed to increasing concentrations of rCNTs and the genome-wide transcription and gene promoter methylation were assessed at three consecutive time points. The results suggest dynamic molecular adaptation with a rapid response in the gene expression and contribution of DNA methylation in the long-term adaptation. Moreover, our analytical approach is able to highlight patterns of molecular alteration *in vitro* that are relevant for the pathogenesis of pulmonary fibrosis, a known long-term effect of rCNTs exposure *in vivo*.

1. Introduction

The immunotoxic potential of multi-walled carbon nanotubes (MWCNTs) on the respiratory system has already been reported with the support of toxicogenomics evidence (Halappanavar et al., 2019; Labib et al., 2016; Kinaret et al., 2017a, 2017b; Poulsen et al., 2017; Rydman et al., 2014). Furthermore, we have recently demonstrated that analyzing the transcriptome from *in vitro* as well as *in vivo* exposures can successfully inform on relevant patterns of molecular adaptation, possible toxic outcomes, and inflammatory responses (Kinaret et al., 2017a). While the use of toxicogenomics in the assessment of adverse effects of chemical exposures is gaining acceptance, chemical risk assessment still largely relies on expensive and laborious animal experiments. *In vitro* models are increasingly used in compliance with the 3R principles (Replacement, Reduction and Refinement) of animal experimentation (Russell and Burch, 1959). Although long-term effects have been investigated *in vitro* [*e.g.* (Comfort et al., 2014; He et al., 2016; Holmgren et al., 2014; Luanpitpong et al., 2014; Wang et al., 2011)], they typically require weeks to months of continuous exposure, hardly cutting back on the time and effort. While recent developments in toxicogenomics can support more advanced interpretation of toxic mechanisms also from *in vitro* models, we are still lacking robust methods for the interpretation of potential long-term effects from short-term assays.

Alterations in DNA methylation have been suggested as a mechanism

* Corresponding author at: Faculty of Medicine and Health Technology, Tampere University, 33520 Tampere, Finland.
E-mail address: dario.greco@tuni.fi (D. Greco).
[1] Authors contributed equally.

https://doi.org/10.1016/j.impact.2020.100274
Received 3 July 2020; Received in revised form 2 November 2020; Accepted 10 November 2020
Available online 19 November 2020

of more persistent molecular changes upon engineered nanomaterials (ENMs) exposures (Brown et al., 2016; Öner et al., 2017; Scala et al., 2018a; Stapleton et al., 2018; Sierra et al., 2017). More recently, multi-omics approaches have been used to explain the complex patterns of molecular adaptation to ENMs in multiple cell types (Scala et al., 2018a). Hence, we hypothesize that relevant information on possible long-term effects of MWCNT can be obtained in a short *in vitro* exposure set-up, by combining the analysis of dynamic gene expression changes with epigenetic alterations that are more stable by nature.

The airways are one of the most prominent routes of exposure to ENMs, making resident lung cell types a valid model for assessing the toxicity of ENMs *in vitro* (Kinaret et al., 2017a; Scala et al., 2018a; Stoccoro et al., 2017; Søs Poulsen et al., 2013). Resident macrophages, together with neutrophils, represent the first line of defense against pathogens and foreign bodies introduced into the airways (Farrera and Fadeel, 2015). These phagocytic cells attempt to internalize the foreign intruders initiating defense mechanisms that can lead to inflammation and, further, damage the tissue when unresolved. Many ENMs are, however, rather biodurable, making their enzymatic degradation a difficult task for phagocytes (Liu et al., 2010; Vlasova et al., 2016). Furthermore, many rigid fiber-like particles are difficult to engulf due to their high aspect-ratio, often leading to impaired ingestion and frustrated phagocytosis that further aggravates inflammation and contributes to the adverse consequences of ENMs exposures (Boyles et al., 2015a; Murphy et al., 2012; Rydman et al., 2014). Moreover, recent evidence suggests that ENMs can impact macrophage polarization, thus affecting the long-term outcome of the exposure (Dong and Ma, 2018; Meng et al., 2015; Kinaret et al., 2020). Although the role of macrophages in reactions induced by carbon nanotubes (CNTs) is recognized, the dynamic patterns of molecular adaptation of macrophages to MWCNTs are yet to be discovered (Kinaret et al., 2017b; Rydman et al., 2014).

To date, dose-dependent molecular responses have been investigated by focusing on individual time points of exposure (Bourdon et al., 2013; Labib et al., 2016). This approach, however, makes the interpretation of the kinetics of molecular adaptation difficult. To overcome this limitation, we applied a novel computational approach that allows the modelling of dynamic dose-dependent (DDD) alterations in two distinct molecular layers, the transcriptome and the DNA methylome (Serra et al., 2020). We applied this analytical strategy in order to model a robust dynamic mechanism of action of MWCNTs on a human macrophage cell model. We exposed macrophage-like cells derived from the human monocytic THP-1 cell line to three different doses (5, 10 and 20 μg/mL) of long and rigid multi-walled carbon nanotubes (rCNTs) for three consecutive time points: 24, 48, and 72 h. We then investigated the DDD molecular alterations at the level of the transcriptome and gene promoter methylation. In this way, we were able to underline key molecular changes already described in lung fibrosis *in vivo*. Our approach supports the use of toxicogenomics in building more comprehensive predictions about the long-term effects of ENMs exposure, such as fibrosis, by using an *in vitro* exposure setup.

2. Material and methods

2.1. Nanomaterial

The multi-walled carbon nanotubes used in this study have been previously characterized in Rydman et al. and Kinaret et al. (Kinaret et al., 2017b; Rydman et al., 2015). The properties of the nanomaterial are summarized in Table 1.

2.2. Cell culture and exposures

THP-1 cells (DSMZ ACC 16) were cultured at 37 °C in cell culture flasks in RPMI 1640 media (Gibco, Thermo Fisher Scientific, USA) with 10% FBS (Gibco), 2 mM ultraglutamine (Gibco), and 1% penicillin-streptomycin (Gibco) supplementation (complete RPMI media). Cells were plated into six-well plates ($1.0 \times 10\hat{}6$ cells/well) and differentiated for 48 h with 50 nM PMA (phorbol 12-myristate 13-acetate, Merck KGaA, Darmstadt, Germany). Fresh, complete RPMI media with PMA was replaced after 24 h and after a total of 48 h, fresh complete media without PMA was added. The control group was treated in a similar manner, with complete media and PMA, without the rCNTs.

Dispersion of the rCNTs was based on publications by Bihari et al. (Bihari et al., 2008) and Gallud et al. (Gallud et al., 2020), and successfully used in several previous publications by us and others (Boyles et al., 2015b; Chortarea et al., 2019; Kinaret et al., 2017a; Kinaret et al., 2020; Scala et al., 2018a). A stock solution of 1 mg/mL of rCNTs was freshly prepared prior to exposure in a sterile glass tube with plain RPMI 1640 media, vortexed for 1 min and sonicated in a bath sonicator (37 kHz, Elmasonic S30 (H), Ilabequipment, USA) for 3×15 min at room temperature. The stock solution was then diluted with complete RPMI media to obtain final exposure concentrations of 5, 10, and 20 μg of rCNT/mL (corresponding to mass per area exposure concentrations of 1.04, 2.08 and 4.16 μg/cm^2 as a total volume of 2 ml of exposure media was used). The dose range was selected to reflect low-dose exposures that are high enough to induce a response without showing significant cytotoxicity (Scala et al., 2018a). The dilutions were vortexed and sonicated prior to exposures for additional 15 mins. Cells (passage number P8) were exposed to rCNTs in complete RPMI for 24, 48 or 72 h. Cells treated in a similar manner, sonicated and RPMI media vortexed in the same way but without rCNTs exposure were used as a reference group. A total of 6 replicates of each treatment and dose pair were performed. After exposures, two replicates were pooled into one sample to produce a total of 3 independent replicates for each exposure group. These triplicates were then used for the following transcriptomics and DNA methylation experiments.

2.3. RNA/DNA extraction

Following each exposure period, the cells were harvested, and lysed, and total RNA was isolated using RNeasy Mini kit (Qiagen, Germany) following the instructions of the manufacturer. Total RNA samples were quantified with NanoDrop (ND-1000, Thermo Fisher Scientific) and the quality of the RNA was further verified using FragmentAnalyzer (Agilent Technologies, USA). RNA samples with RNA quality number (RQN) higher than 9.5 were used for the analysis.

DNA was extracted from the cell lysates using Maxwell® RSC Cultured Cells DNA Kit and the Maxwell® RSC instrument according to manufacturer's instructions (Promega Corporation, USA). Integrity of the DNA was verified by gel electrophoresis on 1% precasted *E*-gel (Invitrogen, Thermo Fisher Scientific) and quantified using PicoGreen (Quant-iT Broad-Range dsDNA Assay Kit, Invitrogen).

Table 1
Characteristics of the multi-walled carbon nanotubes used in the experiment.

Description	Product code	Provider	Aspect ratio	Average length [nm]	Average diameter [nm]	Average surface area [m^2/g]
Rigid multi-walled carbon nanotube	XNRI-7 mitsui	Mitsui & Co., Ltd. (Japan)	260	13,000	50	22

2.4. DNA microarrays

Total RNA samples (100 ng) were labeled and amplified using the T7 RNA polymerase amplification method (Low Input Quick Amp Labeling Kit, Agilent Technologies) following the instructions of the manufacturer (Agilent Technologies). cRNA samples labeled with either Cy3 or Cy5 fluorescent labels (Agilent Technologies) were purified with RNeasy Mini Kit (Qiagen). The quantity and specific activity of the samples were verified using NanoDrop (ND-2000, Thermo Fisher Scientific). Finally, 300 ng of cRNA labeled with Cy3 were combined with a corresponding amount of cRNA labeled with Cy5, fragmented, and hybridized onto the Agilent SurePrint G3 Human GE 8 × 60 microarrays. After washing, the slides were scanned with Agilent microarray scanner model G2505C (Agilent Technologies). Data were extracted using the Agilent Feature Extraction software (V12.0.2.2). Microarray data have been submitted to NCBI Gene Expression Omnibus (GEO) database under the series accession number GSE146710.

2.5. Genome-wide DNA methylation

Genome-wide DNA methylation analysis was performed using the Infinium HD methylation assay (Illumina, USA) according to manufacturer's protocol. First, DNA samples (500 ng) were bisulfite converted using the EZ-96 Methylation Kit (Zymo Research, USA) following the instructions of the manufacturer. Next, DNA was amplified, fragmented, and hybridized to the Infinium MethylationEPIC BeadChips, and finally, scanned with the iScan scanner (Illumina).

2.6. Transcriptomics

Transcriptomics data were preprocessed using the R Shiny application eUTOPIA (Marwah et al., 2019). Raw data were imported, and low-quality probes were filtered out using a quantile-based approach. Particularly, probes with a value higher than 75% quantile of negative probes in at least 85% of the samples were selected for further steps. The log2 transformed intensity values were then normalized between arrays using quantile normalization. Technical variation resulting from the dye, slide, and the position on the slide were eliminated by batch correction with the ComBat method from the R package sva (Leek et al., 2012). Finally, multiple probes mapped to the same gene symbol were summarized by their median values.

Differential expression between each exposure group (one dose at one time point) and their corresponding control group was estimated by linear models followed by empirical Bayes pairwise comparison as implemented in the R package limma (Ritchie et al., 2015). Corrected batches were included as covariates in the analysis. Genes with a fold change $>|1.5|$ and Benjamini & Hochberg adjusted $p < 0.05$ were considered significantly differentially expressed.

2.7. CpG methylation

Methylation data were preprocessed using eUTOPIA following the workflow of the application (Marwah et al., 2019). Raw methylation files were uploaded together with the phenotype file. CpG probes were filtered by removing probes with a detection p-value >0.01 in any sample. Further filtering was applied to remove probes for CpGs located on the sex chromosomes, those containing single nucleotide polymorphisms or belonging to a set of known cross-hybridizing probes (Chen et al., 2013). Data were normalized using the Subset-quantile Within Array Normalization (SWAN) method (Maksimovic et al., 2012). Batch correction was performed with the Combat method from the R package sva to remove technical variation associated to the chip (Leek et al., 2012). Finally, a gene promoter region was defined as 200 bp upstream from the transcription start site of each gene, and the M-values for CpG probes in the promoter region were summarized by their median value for each gene. M-values were transformed into Beta-values using the function m2beta from the R package lumi (Du et al., 2008).

Differential methylation analysis was performed with the limma approach as described above for transcriptomics (Ritchie et al., 2015). The gene promoter was considered significantly differentially methylated with a fold change $>|1.2|$ and $p < 0.01$.

2.8. Dose- and time modelling

Each molecular layer was analyzed separately with parallel approaches following the workflow of TinderMIX (Serra et al., 2020). In brief, sample-wise fold changes were calculated between each exposed sample and each of its corresponding control samples. Fold-changes were log2 transformed and used for the modelling. For transcriptomics data, two-way ANOVA was applied to identify the genes whose fold change showed variance significantly ($p < 0.01$) associated to dose, time, or the interaction of dose and time. These genes were considered "responsive" and selected for further modelling in both molecular layers. First, a selection of polynomial models (linear, second and third order) were fitted to the known points. The optimal model for each gene was selected based on the lowest Akaike Information Criterion (AIC) value, and the genes with a non-significant p-value (FDR corrected $p > 0.05$) for the fitting were filtered out. Afterwards, the dose and time ranges were divided into 50 equally distributed bins, and the optimal model of each gene was used to predict their corresponding log2 fold changes. In such a way, each gene is represented by a 50 by 50 activation map in the space of time and dose, that is able to interpolate the doses and time points not included in the experiment. From each activation map, an area with monotonically increasing or decreasing (with respect to the dose) fold change greater than the activity threshold (fold change$>|1.1|$) was recognized by means of its gradient matrix and determined as "responsive area". If such an area could be identified, the gene was considered to be altered in dynamic dose-responsive manner. Finally, the activation map was divided into three equal sections on the time axis and each section was assigned a label: "early", "middle", and "late", respectively, according to the implementation of the TinderMIX software (Serra et al., 2020). With this approach, each gene was assigned one of these labels based on the time of activation of the gene, *i.e.* the section in which the activity threshold was surpassed at the earliest time point and the lowest possible dose.

2.9. Functional enrichment

Pathway enrichments were performed using an R-shiny graphical tool FunMappOne (Scala et al., 2019). Lists of official gene symbols were offered as an input with the direction of the alteration (fold-change increasing or decreasing with dose) as a modification of the genes. Reactome annotations were used for pathway enrichment, and all known genes were used as the statistical domain scope of the analysis. Pathways were considered significantly enriched with a p-value <0.01 adjusted with the g:SCS method (Reimand et al., 2007).

3. Results and discussion

Given the important role of macrophages in the systemic responses to ENMs exposure, we decided to focus on a macrophage *in vitro* model. We aimed at disentangling the kinetics of the molecular adaptation by using a multi-omics approach in combination with multiple time points and rCNTs doses showing low toxicity (Scala et al., 2018a).

3.1. Transcriptional changes follow a dose-dependent trend

Differential expression is often used to statistically evaluate the quantitative transcriptomic changes between experimental groups. Exposing macrophages to increasing concentrations of rCNTs for three consecutive time points resulted in a total of 5495 differentially

expressed genes (DEGs) (Table S1). A clear dose-dependent increase in the number of DEGs can be visually observed at each time point, suggesting a more impactful exposure as the dose increases (Fig. 1A). On the contrary, the number of differentially methylated promoters (DMPs) only showed a visually increasing dose-dependent trend at 24 h and a dose-dependently decreasing number of hypomethylated promoters was observed at 48 h (Fig. 1B). Total of 307 gene promoter regions showed significant differential methylation as compared to unexposed controls. The subtle impact on DNA methylation observed in the present study is in line with previous reports suggesting limited changes of the methylation levels in fewer *loci* upon exposure to MWCNTs (Öner et al., 2017; Scala et al., 2018a; Sierra et al., 2017). However, we observed a convincing pattern of DNA methylation adaptation at the highest dose and the longest exposure time with a higher prevalence of hypomethylated promoters (Fig. 1B). While the gene expression is regulated by dynamic mechanisms, such as transcription factor binding, regulation of the enzymatic machineries controlling DNA methylation is slower and also involves cell replication -dependent events (Edwards et al., 2017). For this reason, we cannot exclude that some of the regulatory mechanisms of DNA methylation are not active in a differentiated cell type/cell culture, where cell cycle is largely halted. This might be progressively evident as the exposure time proceeds through the 72 h.

3.2. Dynamic dose-dependent analysis highlights an additional set of adaptive genes

The conventional analysis of differential expression/methylation by comparing treated to non-treated samples follows the observations of several previous studies indicating a prominent transcriptomic response but a marginal impact on the DNA methylation (Kinaret et al., 2017a; Öner et al., 2017; Scala et al., 2018a; Sierra et al., 2017). We suspected that part of the molecular effects are directly induced by the chemical agents and substances and thus, show dose-dependent behavior. Hence, we focused on finding the genes whose behavior is monotonically altered with an increasing dose. Benchmark dose (BMD) modelling has been proposed to identify such genes (Yang et al., 2007). Although BMD modelling succeeds in highlighting monotonically altered genes, it gives little insight into the kinetics of the molecular alteration. Here, we investigated the DDD behavior of the genes upon rCNTs exposure by simultaneously modelling the effects of the dose and time. With this integrated approach, we obtained a total of 6428 genes with DDD alteration in gene expression and 414 genes with DDD changes in the promoter methylation. The genes with DDD behavior were labeled "early", "middle", or "late" based on their point of departure (POD) in each distinct molecular layer (Table 2, Table S2). Interestingly, the kinetics of the molecular alterations showed distinct patterns in each molecular layer, as the majority of the changes in gene expression were initiated early, while alterations in the promoter methylation were mostly observed at late exposure time (Table 2). Given the more stable, regulatory nature of DNA methylation, later activation is expected. Evidence of later changes in DNA methylation has also been shown *in vivo*, as significant changes in DNA methylation levels in the lungs of mice exposed to MWCNTs were observed 7 days after the exposure, but not at 24 h (Brown et al., 2016).

Table 2
Number of dynamic dose-dependent molecular alterations obtained for gene expression and gene promoter regions, specified by their time of activation.

Activation time/Molecular layer	Early	Middle	Late	Total
Expression	3912	1092	1424	6428
Methylation	131	44	239	414

By comparing the differentially expressed genes and differentially methylated promoters with the respective set of DDD genes, we found an intersection of 3212 (58%) genes for expression (Fig. 2A), and an intersection of 70 (23%) promoters for methylation (Fig. 2B), respectively. As we suspected, these results suggest that the mechanism of action of rCNTs is only partially dose-dependent, with 58% of DEGs showing dose-dependent behavior, while molecular adaptation as a whole is achieved, not surprisingly, by complex circuits of non-monotonic molecular regulation. Furthermore, our approach identified a large proportion of molecular alterations not captured by the traditional differential expression/methylation analysis (Fig. 2A-B). Our integrated dose- and time- modelling approach allows us to retrieve also genes whose magnitude of alteration could not be sufficiently evident in each exposed *vs* control pairwise comparison. Furthermore, the investigation of the POD is especially useful in the regulatory setting for example in defining toxicological reference doses (Labib et al., 2016; Webster et al., 2015).

3.3. A proportion of dynamic dose-dependent genes are coupled with dose-dependent alteration also in the gene promoter methylation

The assessment of alterations in DNA methylation can be useful for predicting long-term effects of short-term exposures (Canzler et al., 2020). In order to understand the relationship between transcriptional and epigenetic adaptation, we investigated the two molecular layers in relation to each other. In total, the two layers shared 220 DDD genes (3.4% of all the DDD transcriptionally altered genes) (Fig. 3A, Table S3). These results are in line with our previous findings suggesting that only a proportion of genes acquire "more stable" molecular alteration in the form of DNA methylation (Scala et al., 2018a). When considering the

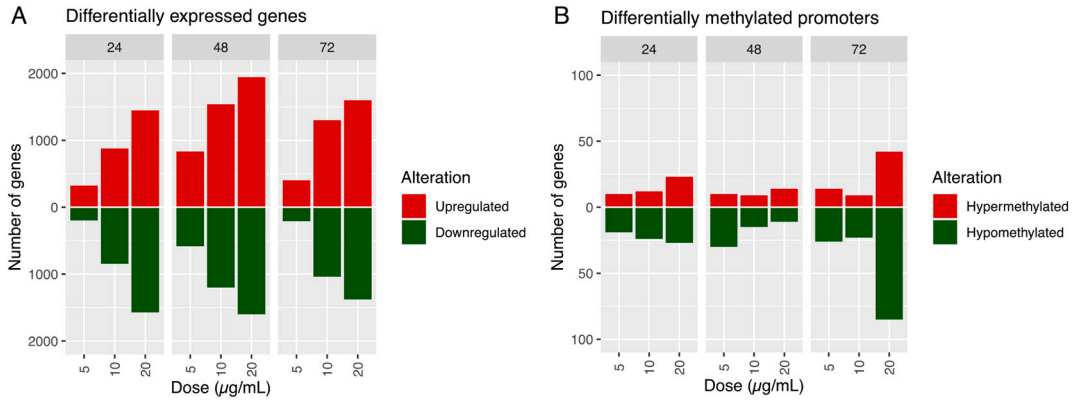

Fig. 1. Number of genes altered in respect to rCNTs exposure. Timepoints 24, 48 and 72 h of exposure with 5, 10 and 20 μg/mL exposure concentrations (Dose). (A) Differentially expressed genes with bars representing number of up- (red) and down- (green) regulated genes for expression (FC > |1.5|, FDR-corrected *p*-value <0.05) (B) and hyper- (red) and hypomethylated (green) promoters for differential methylation (FC > |1.2|, *p*-value <0.01), respectively. (For interpretation of the references to colour in this figure legend, the reader is referred to the web version of this article.)

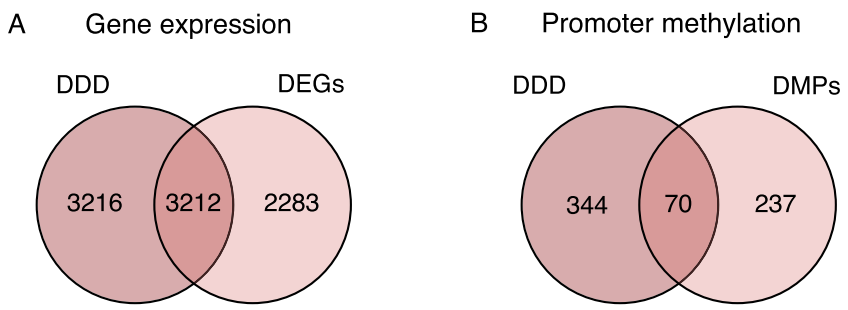

Fig. 2. Venn diagrams representing the overlap of genes obtained through the modelling of dynamic dose-dependent (DDD) alterations and standard analysis of differentially expressed genes (DEGs) (A) or differentially methylated promoters (DMPs) (B).

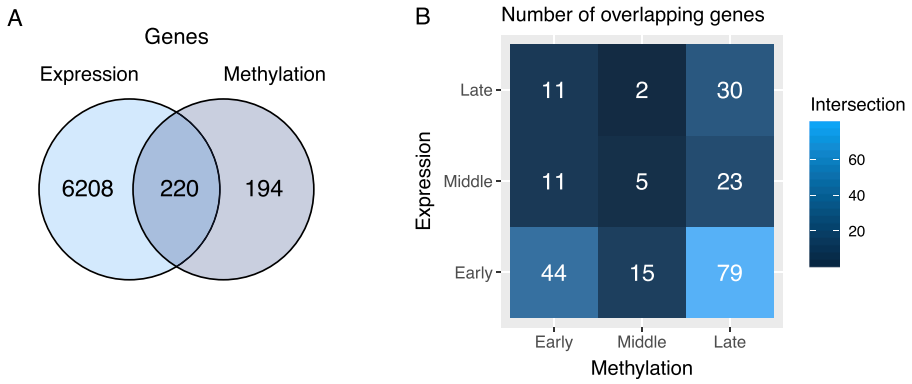

Fig. 3. Intersections between gene expression and promoter methylation at the level of all DDD genes (A) and the overlapping DDD genes and promoter regions grouped by activation time (B).

kinetics of these molecular alterations, we found the largest overlap (79 genes) between genes whose expression alteration was initiated early while methylation perturbation was triggered late, suggesting the role of DNA methylation in sustaining or repressing these expression patterns long-term (Fig. 3B).

The 220 common genes indicate several important macrophage functions to be affected by epigenetic regulation in response to rCNTs. Among the set of common genes, in fact, we identified multiple chemokine encoding genes that have a pivotal role in macrophage induced inflammation (Table S3). For instance, CXCL8, CXCL10, and CCL20 were upregulated, while their promoters were hypomethylated, suggesting a sustained long-term induction of these genes. We also observed altered behavior of several genes indicating calcium homeostasis, as the transcription of the calcium channel genes CACFD1, CACNA2D1, CACNA2D4, CACNG2 was repressed, while their promoters were generally hypermethylated. Downregulation of genes encoding for calcium channels could indicate an increased level of cytosolic calcium, which in turn triggers multiple signaling pathways in activated macrophages, including IL-1β secretion and the activation of NLRP3 inflammasome (Feske et al., 2015; Rada et al., 2014; Zumerle et al., 2019). Indeed, nano-sized particles have been shown to modulate intracellular calcium concentration, and exposure to long and rigid MWCNTs has been previously associated with NLRP3 inflammasome activation (Brown et al., 2004; Li et al., 2017; Palomäki et al., 2011). Both of these events are reported to be dependent on reactive oxygen species (ROS) production, which is also known to be acutely induced in our experimental setup (Scala et al., 2018a). Taken together, these results suggest the role of methylation in sustaining selected patterns of transcriptional adaptation of macrophages to rCNTs exposure.

3.4. DDD alterations in transcription and methylation are related to cell activation and homeostasis

To better understand the functionality of the DDD genes in each molecular layer, we investigated the enriched pathways in each group. Our analysis highlighted a total of 493 significantly enriched Reactome pathways for gene expression and 68 pathways for promoter methylation. Out of these, 63 pathways (13%) were shared between the two molecular layers (Fig. 4A). All the common enriched pathways were activated early in the transcriptome with a great proportion (68%) of them sustaining the enrichment along the time (Fig. 4B). Pathways such as “immune system”, “disease”, “signal transduction”, “metabolism” and “cell cycle” represent many of the functions already highlighted by earlier toxicogenomic studies both in vitro and in vivo (Kinaret et al., 2017a, 2017b; Öner et al., 2017; Poulsen et al., 2017; Scala et al., 2018a).

We found several key pathways of the immune functions to be prominently represented, including well known responses of macrophages to MWCNTs exposure, such as *innate immune response*, *inflammation*, *cytokine signaling*, and *antigen processing and presentation* (Fig. 4B) (Kinaret et al., 2017a, 2017b; Poulsen et al., 2017; Scala et al., 2018a). Previous studies have also reported epigenetic regulation of these processes in response to MWCNTs (Öner et al., 2017; Scala et al., 2018a). Interestingly, in methylation, *immune system* was the only pathway already enriched at “middle” and sustaining it at “late”, suggesting a more pronounced role of promoter methylation in the regulation of immune-related genes. The combination of alterations in transcription and promoter methylation suggests long-term regulation of the genes of these pathways. While the enrichment of immune related functions is not surprising considering the nature of the exposure, it indicates that our analytical approach is able to highlight short- and possible long-term patterns relevant for the exposure. In addition, several compartments of the cell metabolism were found to be altered, including *response to stress*

Fig. 4. (A) Venn diagram representing the intersection of all enriched Reactome pathways for genes with DDD expression and promoter regions with DDD methylation. (B) Heatmap representing the enrichment patterns of the 63 Reactome pathways common to gene expression and promoter methylation.

as well as *protein and RNA metabolic processes* (Fig. 4B). Alteration of general metabolic pathways could indicate cellular stress, while functions related to protein metabolism may support well known macrophage functions, such as antigen processing and presentation. The role of epigenetic alteration in protein metabolic processes observed in this study, have been also reported previously (Öner et al., 2017; Scala et al., 2018b).

The most represented common functions in this study were related to signaling pathways. We have previously observed a pronounced positive association between the alteration of intracellular signaling pathways and the nanoparticle aspect ratio (Scala et al., 2018a). Similar patterns of alterations have been reported at the level of the transcriptome *in vivo* as well as DNA methylation *in vitro* (Kinaret et al., 2017a, 2017b; Öner et al., 2017; Scala et al., 2018a). Here, our results highlight the activation of *MAPK signaling* pathways, as also previously reported (Kinaret et al., 2017a; Öner et al., 2017; Scala et al., 2018a). MAPK signaling has an important role in regulating innate immune responses as well as cell survival (Arthur and Ley, 2013; Cargnello and Roux, 2011). Interestingly, functions related to epigenetic regulation of gene expression were also retrieved among the pathways commonly represented in both data layers analyzed in this study, supporting the role of DNA methylation and its regulation in the adaptation of macrophages to rCNTs exposure.

3.5. Pathways underlying short-term adaptation are not coupled with promoter methylation changes

When looking at the alterations seen only at the level of the transcriptome, we observed that 79% of the pathways were initiated early and not sustained through time, indicating a rapid short-term macrophage response through transcriptomic alterations (Table S4). As in the common pathways between expression and methylation, immune functions, signaling pathways, and metabolic functions were highly represented in the DDD genes in the transcriptomics layer (Table S4). This suggests that epigenetic regulation of these functions is limited to a small number of genes needed for long-term adaptation. Furthermore, pathways observed only in the transcriptome include acute effects such as apoptosis and DNA damage response indicating a stress response that requires rapid engagement. Even at the sub-toxic concentrations used in the present study, rCNTs exposure is known to exert cellular stress, also observed here by the induction of apoptotic pathways, downregulation of cellular metabolism, and activation of DNA repair pathways (Kinaret et al., 2017a; Scala et al., 2018a; Srivastava et al., 2011).

Furthermore, we identified nuclear factor kappa B (NF-κB) signaling in the center of the macrophage transcriptomic response to rCNTs. NF-κB transcription factors rapidly regulate a wide array of genes involved in immune functions and inflammation, and NF-κB signaling can be activated by various *stimuli* (Liu et al., 2017). The canonical NF-κB signaling pathway activation is associated to several proinflammatory cytokines and pattern recognition receptors (PRRs), such as Toll-like receptors (TLRs). Instead, the non-canonical pathway is generally activated through tumor necrosis factor (TNF) receptor superfamily members (Liu et al., 2017; Sun, 2017). Mukherjee et al. recently suggested NF-κB signaling as a central regulator of transcriptional responses to single-walled carbon nanotubes (SWCNTs) *via* a direct interaction with TLRs (Mukherjee et al., 2018). Of note, while TLR pathways are consistently found to be enriched in response to MWCNTs exposure, including this study (Table S4), direct physical interaction is reported in literature only between SWCNTs and TLRs (Mozolewska et al., 2015; Mukherjee et al., 2018). Considering the bigger diameter of MWCNTs particles (up to 50 times larger than SWCNTs), the interaction between different sized and shaped CNTs and TLRs might differ. In contrast to the canonical NF-κB signaling induced by SWCNTs, our study highlights early activation of *TNFR2 non-canonical NF-kB pathway* (Table S4), suggesting distinct modes of NF-κB signaling activation between different types of CNTs. Furthermore, our analysis showed an early induction of key genes of the non-canonical NF-κB signaling, including both subunits of the p52/RelB complex alongside several possible initiating molecules (*e.g.* CD40 and TNF), as well as the central signaling component of the non-canonical NF-κB pathway, MAP3K14 (Table S2) (Sun, 2017).

3.6. Macrophage molecular adaptation to rCNTs comprises alterations recapitulating mechanisms leading to lung fibrosis

Pulmonary fibrosis is one of the best characterized pathologies associated to CNTs exposures (Dong et al., 2015; Labib et al., 2016; Nikota et al., 2017; Sun et al., 2015). Although the development of pulmonary fibrosis is a complex process orchestrated by various cell types in the lung tissue, macrophages have a pivotal role in the initiation of the steps towards its development. While the complete set of MWCNTs-induced pathological alterations leading to fibrosis in the lung is still to be clarified, the early contribution of acute inflammation and ROS production has been already elucidated (Dong et al., 2015; Labib et al., 2016; Li et al., 2017). The increase of ROS production affects various cell types, and the inflammation promoting response in macrophages, specifically through NF-κB signaling, guides the biological system towards a fibrogenic response (He et al., 2011). Indeed, our results also highlight NF-κB activation (*cfr*. Paragraph 3.5 and Table S4). This type of signaling from macrophages is essential for the development of fibrosis, as the molecules secreted by macrophages regulate the function of other cell types, namely fibroblasts, in the tissue. In addition to NF-κB signaling, other signaling pathways are also relevant. For instance, TGF-b signaling, AKT/mTOR signaling, and WNT signaling, whose role in fibrosis has been extensively reviewed elsewhere (He and Dai, 2015), play a key role in the pathogenesis of fibrosis. All of these signaling pathways were found significantly enriched in our results (Table S4), and some of the key genes involved in these signaling pathways are represented in Fig. 5. Furthermore, recent evidence suggests that CNTs induce alternative macrophage activation both *in vivo* and *in vitro* (Dong and Ma, 2018; Meng et al., 2015; Kinaret et al., 2020). Mixed status of pro-inflammatory, M1-type and healing/regulatory M2-type macrophage activation has been associated to CNTs-induced fibrosis *in vivo* (Dong and Ma, 2018). Our observation on the induction of genes encoding for proinflammatory factors, such as IL-1β, CXCL-8, and TNF, suggest M1 activation, whereas the upregulation of profibrogenic mediators such as PDGFA, TGF-β2, VEGF-A, and CTGF together with anti-inflammatory IL-10, suggest the activation of M2-macrophages (Fig. 5, Table S2). The imbalanced combination of prolonged inflammation and persistent activation of M2-macrophages suggest pathogenesis of fibrosis (Dong and Ma, 2018; Braga et al., 2015). Interestingly, a further comparison of the DDD genes with known, rCNT-induced genes associated to lung fibrosis in an *in vivo* murine model, resulted in 55 common genes (out of 138) (Nikota et al., 2017). Altogether, these results suggest that our *in vitro* model of macrophage exposure is able to highlight relevant patterns of molecular alterations associated to the development of pulmonary fibrosis.

The involvement of DNA methylation in the progression of pulmonary fibrosis caused by MWCNTs has also been postulated (Brown et al., 2016). Indeed, we observed an early transcriptional induction and late promoter hypomethylation of the pulmonary fibrosis marker MMP-7 as well as the already mentioned CXCL-8, a chemokine associated with chronic inflammatory diseases and fibrosis in the lung (Rosas et al., 2008; Russo et al., 2014). These molecular changes suggest persistent expression of these genes through reduced gene promoter methylation. Our results also highlight DDD genes and gene promoters involved in events known to contribute to the development of fibrosis, such as cellular response to stress, alteration of calcium homeostasis, and protein metabolism in both molecular layers (Fig. 4, Table S4) (Ryan et al., 2014). Moreover, pathways found enriched only in the methylome were related to fibroblast growth factor receptor (FGFR) signaling (Table S4), further suggesting the role of DNA methylation in the macrophage response leading towards fibrosis (Inoue et al., 2002).

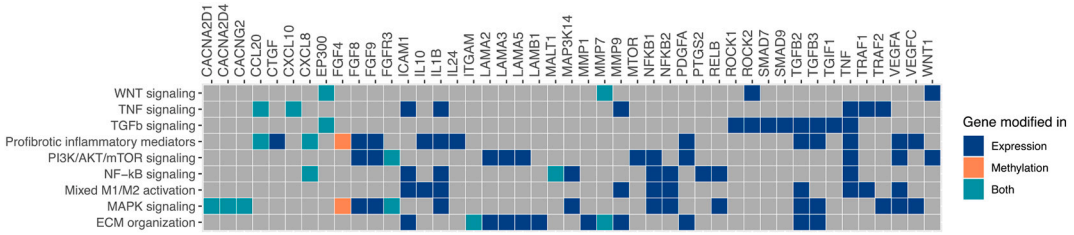

Fig. 5. Pathways and genes relevant to pulmonary fibrosis. Heatmap represents selected genes associated to signaling pathways and biological functions relevant for the pathogenesis of fibrosis. Colored squares denote the association of genes with biological functions. Blue indicates gene to have DDD alteration in expression, orange in methylation and turquoise in both, respectively. (For interpretation of the references to colour in this figure legend, the reader is referred to the web version of this article.)

We have previously shown the potential of *in vitro* strategies coupled with advanced computational methods in informing on relevant outcomes of *in vivo* exposures (Kinaret et al., 2017a). In this study, we further utilized advanced toxicogenomics data modelling to investigate the complex mechanisms of adaptation in response to rCNTs exposure. We used PMA-differentiated THP-1 cells and a combination of multiple doses and time points. With this relatively simple model, we were able to highlight the activation of several well-known fibrosis-related genes and specific activation patterns suggesting potential long-term effects previously described *in vivo*. However, macrophages are a diverse group of cells, and differences between phenotypes and polarization status cannot be neglected (Kinaret et al., 2020). Regulatory bodies and the scientific community are currently putting significant effort to replace animal experiments with as short as possible *in vitro* testing with predictive power. This study brings valuable insights into obtaining evidence of potential long-term consequences from simple *in vitro* models when combined with robust and innovative computational strategies (Kinaret et al., 2017a). While our findings concerning the transcriptomic alterations are in line with multiple reports of CNTs effects on the gene expression, there is less data currently available concerning their ability to alter the DNA methylation. Moreover, the effects of ENMs exposures on other epigenetic mechanisms, including histone modifications, chromosome remodeling, and non-coding RNAs, are even less characterized (Gedda et al., 2019; Yu et al., 2020). Exploring the outcomes of ENMs exposures on these mechanisms can deepen the understanding of their toxicity. The approach used in the present study offers a valuable steppingstone for future integrated studies investigating other molecular alterations and the effects of different exposures.

While modelling the long-term effects from short-term *in vitro* exposures is not a simple task, our multi-omics approach to dynamic dose-dependent alterations is able to highlight macrophage responses both at the level of the transcriptome and methylome, and is able to suggest potential long-term effects already after a 72-h *in vitro* exposure set-up. These findings support the use of combined *in vitro* model systems and toxicogenomics approaches, simultaneously promoting the development of faster, cheaper, and more ethical testing strategies for ENMs.

4. Conclusions

Here, we report alteration of multiple genes and pathways with a key role in macrophage activation in response to rCNTs exposure. Our findings show distinct kinetics of adaptation in the transcriptome and promoter methylation. While macrophages respond at 24 h of exposure by mainly altering gene expression, as the exposure continues through 72 h, epigenetic mechanisms also have a role in macrophage adaptation. Our results convincingly suggest that our toxicogenomic approach of *in vitro* models informs on relevant pathogenic events observed *in vivo*.

Supplementary data to this article can be found online at https://doi.org/10.1016/j.impact.2020.100274.

Declaration of Competing Interest

The authors declare no competing interests.

Acknowledgements

This study received funding from EU H2020 project NanoSolveIT (grant agreement 814572) and the Academy of Finland (grant agreement 322761).

The authors would further like to thank Ilke Daldal for the assistance in the experimental part, Susanna Fagerholm (University of Helsinki) for sharing cell culture facilities with us and Silvia Polidoro (HUGEF) for performing the genome-wide methylation assay.

References

Arthur, J.S.C., Ley, S.C., 2013. Mitogen-activated protein kinases in innate immunity. Nat. Rev. Immunol. 13, 679–692. https://doi.org/10.1038/nri3495.

Bihari, P., Vippola, M., Schultes, S., Praetner, M., Khandoga, A.G., Reichel, C.A., et al., 2008. Optimized dispersion of nanoparticles for biological *in vitro* and *in vivo* studies. Part Fibre Toxicol. 5, 14. https://doi.org/10.1186/1743-8977-5-14.

Bourdon, J.A., Williams, A., Kuo, B., Moffat, I., White, P.A., Halappanavar, S., et al., 2013. Gene expression profiling to identify potentially relevant disease outcomes and support human health risk assessment for carbon black nanoparticle exposure. Toxicology. 303, 83–93. https://doi.org/10.1016/j.tox.2012.10.014.

Boyles, M.S.P., Young, L., Brown, D.M., MacCalman, L., Cowie, H., Moisala, A., et al., 2015a. Multi-walled carbon nanotube induced frustrated phagocytosis, cytotoxicity and pro-inflammatory conditions in macrophages are length dependent and greater than that of asbestos. Toxicol. in Vitro 29, 1513–1528. https://doi.org/10.1016/j.tiv.2015.06.012.

Boyles, M.S.P., Young, L., Brown, D.M., MacCalman, L., Cowie, H., Moisala, A., et al., 2015b. Multi-walled carbon nanotube induced frustrated phagocytosis, cytotoxicity and pro-inflammatory conditions in macrophages are length dependent and greater than that of asbestos. Toxicol. in Vitro 29, 1513–1528. https://doi.org/10.1016/j.tiv.2015.06.012.

Braga, T.T., Agudelo, J.S.H., Camara, N.O.S., 2015. Macrophages during the fibrotic process: M2 as friend and foe. Front. Immunol. 6, 602. https://doi.org/10.3389/fimmu.2015.00602.

Brown, D.M., Donaldson, K., Borm, P.J., Schins, R.P., Dehnhardt, M., Gilmour, P., et al., 2004. Calcium and ROS-mediated activation of transcription factors and TNF-alpha cytokine gene expression in macrophages exposed to ultrafine particles. Am. J. Phys. Lung Cell. Mol. Phys. 286, L344–L353. https://doi.org/10.1152/ajplung.00139.2003.

Brown, T.A., Lee, J.W., Holian, A., Porter, V., Fredriksen, H., Kim, M., et al., 2016. Alterations in DNA methylation corresponding with lung inflammation and as a biomarker for disease development after MWCNT exposure. Nanotoxicology. 10, 453–461. https://doi.org/10.3109/17435390.2015.1078852.

Canzler, S., Schor, J., Busch, W., Schubert, K., Rolle-Kampczyk, U.E., Seitz, H., et al., 2020. Prospects and challenges of multi-omics data integration in toxicology. Arch. Toxicol. 94, 371–388. https://doi.org/10.1007/s00204-020-02656-y.

Cargnello, M., Roux, P.P., 2011. Activation and function of the MAPKs and their substrates, the MAPK-activated protein kinases. Microbiol. Mol. Biol. Rev. 75, 50–83. https://doi.org/10.1128/MMBR.00031-10.

Chen, Y., Lemire, M., Choufani, S., Butcher, D.T., Grafodatskaya, D., Zanke, B.W., et al., 2013. Discovery of cross-reactive probes and polymorphic CpGs in the Illumina Infinium HumanMethylation450 microarray. Epigenetics. 8, 203–209. https://doi.org/10.4161/epi.23470.

Chortarea, S., Zerimariam, F., Barosova, H., Septiadi, D., Clift, M.J.D., Petri-Fink, A., et al., 2019. Profibrotic activity of multiwalled carbon nanotubes upon prolonged exposures in different human lung cell types. Appl. In Vitro Toxicol. 5, 47–61. https://doi.org/10.1089/aivt.2017.0033.

Comfort, K.K., Braydich-Stolle, L.K., Maurer, E.I., Hussain, S.M., 2014. Less is more: long-term in vitro exposure to low levels of silver nanoparticles provides new insights for

nanomaterial evaluation. ACS Nano 8, 3260–3271. https://doi.org/10.1021/nn5009116.
Dong, J., Ma, Q., 2018. Macrophage polarization and activation at the interface of multi-walled carbon nanotube-induced pulmonary inflammation and fibrosis. Nanotoxicology. 12, 153–168. https://doi.org/10.1080/17435390.2018.1425501.
Dong, J., Porter, D.W., Batteli, L.A., Wolfarth, M.G., Richardson, D.L., Ma, Q., 2015. Pathologic and molecular profiling of rapid-onset fibrosis and inflammation induced by multi-walled carbon nanotubes. Arch. Toxicol. 89, 621–633. https://doi.org/10.1007/s00204-014-1428-y.
Du, P., Kibbe, W.A., Lin, S.M., 2008. Lumi: a pipeline for processing Illumina microarray. Bioinformatics 24, 1547–1548. https://doi.org/10.1093/bioinformatics/btn224.
Edwards, J.R., Yarychkivska, O., Boulard, M., Bestor, T.H., 2017. DNA methylation and DNA methyltransferases. Epigenetics Chromatin 10, 23. https://doi.org/10.1186/s13072-017-0130-8.
Farrera, C., Fadeel, B., 2015. It takes two to tango: understanding the interactions between engineered nanomaterials and the immune system. Eur. J. Pharm. Biopharm. 95, 3–12. https://doi.org/10.1016/j.ejpb.2015.03.007.
Feske, S., Wulff, H., Skolnik, E.Y., 2015. Ion channels in innate and adaptive immunity. Annu. Rev. Immunol. 33, 291–353. https://doi.org/10.1146/annurev-immunol-032414-112212.
Gallud, A., Delaval, M., Kinaret, P., Marwah, V.S., Fortino, V., Ytterberg, J., et al., 2020. Multiparametric profiling of engineered nanomaterials: unmasking the surface coating effect. Adv. Sci. 2002221 https://doi.org/10.1002/advs.202002221.
Gedda, M.R., Babele, P.K., Zahra, K., Madhukar, P., 2019. Epigenetic aspects of engineered nanomaterials: is the collateral damage inevitable? Front. Bioeng. Biotechnol. 7, 228. https://doi.org/10.3389/fbioe.2019.00228.
Halappanavar, S., Rahman, L., Nikota, J., Poulsen, S.S., Ding, Y., Jackson, P., et al., 2019. Ranking of nanomaterial potency to induce pathway perturbations associated with lung responses. NanoImpact. 14, 100158. https://doi.org/10.1016/j.impact.2019.100158.
He, W., Dai, C., 2015. Key Fibrogenic Signaling. Curr. Pathobiol. Rep. 3, 183–192. https://doi.org/10.1007/s40139-015-0077-z.
He, X., Young, S.-H., Schwegler-Berry, D., Chisholm, W.P., Fernback, J.E., Ma, Q., 2011. Multiwalled carbon nanotubes induce a fibrogenic response by stimulating reactive oxygen species production, activating NF-κB signaling, and promoting fibroblast-to-myofibroblast transformation. Chem. Res. Toxicol. 24, 2237–2248. https://doi.org/10.1021/tx200351d.
He, X., Despeaux, E., Stueckle, T.A., Chi, A., Castranova, V., Dinu, C.Z., et al., 2016. Role of mesothelin in carbon nanotube-induced carcinogenic transformation of human bronchial epithelial cells. Am. J. Phys. Lung Cell. Mol. Phys. 311, L538–L549. https://doi.org/10.1152/ajplung.00139.2016.
Holmgren, G., Sjögren, A.-K., Barragan, I., Sabirsh, A., Sartipy, P., Synnergren, J., et al., 2014. Long-term chronic toxicity testing using human pluripotent stem cell-derived hepatocytes. Drug Metab. Dispos. 42, 1401–1406. https://doi.org/10.1124/dmd.114.059154.
Inoue, Y., King, T.E., Barker, E., Daniloff, E., Newman, L.S., 2002. Basic fibroblast growth factor and its receptors in idiopathic pulmonary fibrosis and lymphangioleiomyomatosis. Am. J. Respir. Crit. Care Med. 166, 765–773. https://doi.org/10.1164/rccm.2010014.
Kinaret, P., Marwah, V., Fortino, V., Ilves, M., Wolff, H., Ruokolainen, L., et al., 2017a. Network analysis reveals similar transcriptomic responses to intrinsic properties of carbon nanomaterials in vitro and in vivo. ACS Nano 11, 3786–3796. https://doi.org/10.1021/acsnano.6b08650.
Kinaret, P., Ilves, M., Fortino, V., Rydman, E., Karisola, P., Lähde, A., et al., 2017b. Inhalation and oropharyngeal aspiration exposure to rod-like carbon nanotubes induce similar airway inflammation and biological responses in mouse lungs. ACS Nano 11, 291–303. https://doi.org/10.1021/acsnano.6b05652.
Kinaret, P.A.S., Scala, G., Federico, A., Sund, J., Greco, D., 2020. Carbon nanomaterials promote M1/M2 macrophage activation. Small e1907609. https://doi.org/10.1002/smll.201907609.
Labib, S., Williams, A., Yauk, C.L., Nikota, J.K., Wallin, H., Vogel, U., et al., 2016. Nano-risk science: application of toxicogenomics in an adverse outcome pathway framework for risk assessment of multi-walled carbon nanotubes. Part Fibre Toxicol. 13, 15. https://doi.org/10.1186/s12989-016-0125-9.
Leek, J.T., Johnson, W.E., Parker, H.S., Jaffe, A.E., Storey, J.D., 2012. The sva package for removing batch effects and other unwanted variation in high-throughput experiments. Bioinformatics. 28, 882–883. https://doi.org/10.1093/bioinformatics/bts034.
Li, H., Tan, X.-Q., Yan, L., Zeng, B., Meng, J., Xu, H.-Y., et al., 2017. Multi-walled carbon nanotubes act as a chemokine and recruit macrophages by activating the PLC/IP3/CRAC channel signaling pathway. Sci. Rep. 7, 226. https://doi.org/10.1038/s41598-017-00386-3.
Liu, T., Zhang, L., Joo, D., Sun, S.-C., 2017. NF-κB signaling in inflammation. Signal Transduct. Target. Ther. 2 https://doi.org/10.1038/sigtrans.2017.23.
Liu, X., Hurt, R.H., Kane, A.B., 2010. Biodurability of single-walled carbon nanotubes depends on surface functionalization. Carbon N. Y. 48, 1961–1969. https://doi.org/10.1016/j.carbon.2010.02.002.
Luanpitpong, S., Wang, L., Castranova, V., Rojanasakul, Y., 2014. Induction of stem-like cells with malignant properties by chronic exposure of human lung epithelial cells to single-walled carbon nanotubes. Part Fibre Toxicol. 11, 22. https://doi.org/10.1186/1743-8977-11-22.
Maksimovic, J., Gordon, L., Oshlack, A., 2012. SWAN: subset-quantile within array normalization for illumina infinium HumanMethylation450 BeadChips. Genome Biol. 13, R44. https://doi.org/10.1186/gb-2012-13-6-r44.
Marwah, V.S., Scala, G., Kinaret, P.A.S., Serra, A., Alenius, H., Fortino, V., et al., 2019. eUTOPIA: solUTion for Omics data PreprocessIng and analysis. Source Code Biol. Med. 14, 1. https://doi.org/10.1186/s13029-019-0071-7.
Meng, J., Li, X., Wang, C., Guo, H., Liu, J., Xu, H., 2015. Carbon nanotubes activate macrophages into a M1/M2 mixed status: recruiting naïve macrophages and supporting angiogenesis. ACS Appl. Mater. Interfaces 7, 3180–3188. https://doi.org/10.1021/am507649n.
Mozolewska, M.A., Krupa, P., Rasulev, B., Liwo, A., Leszczynski, J., 2015. Preliminary Studies of Interaction Between Nanotubes and Toll-like Receptors.
Mukherjee, S.P., Bondarenko, O., Kohonen, P., Andón, F.T., Brzicová, T., Gessner, I., et al., 2018. Macrophage sensing of single-walled carbon nanotubes via Toll-like receptors. Sci. Rep. 8, 1115. https://doi.org/10.1038/s41598-018-19521-9.
Murphy, F.A., Schinwald, A., Poland, C.A., Donaldson, K., 2012. The mechanism of pleural inflammation by long carbon nanotubes: interaction of long fibres with macrophages stimulates them to amplify pro-inflammatory responses in mesothelial cells. Part Fibre Toxicol. 9, 8. https://doi.org/10.1186/1743-8977-9-8.
Nikota, J., Banville, A., Goodwin, L.R., Wu, D., Williams, A., Yauk, C.L., et al., 2017. Stat-6 signaling pathway and not Interleukin-1 mediates multi-walled carbon nanotube-induced lung fibrosis in mice: insights from an adverse outcome pathway framework. Part Fibre Toxicol. 14, 37. https://doi.org/10.1186/s12989-017-0218-0.
Öner, D., Moisse, M., Ghosh, M., Duca, R.C., Poels, K., Luyts, K., et al., 2017. Epigenetic effects of carbon nanotubes in human monocytic cells. Mutagenesis. 32, 181–191. https://doi.org/10.1093/mutage/gew053.
Palomäki, J., Välimäki, E., Sund, J., Vippola, M., Clausen, P.A., Jensen, K.A., et al., 2011. Long, needle-like carbon nanotubes and asbestos activate the NLRP3 inflammasome through a similar mechanism. ACS Nano 5, 6861–6870. https://doi.org/10.1021/nn200595c.
Poulsen, S.S., Knudsen, K.B., Jackson, P., Weydahl, I.E.K., Saber, A.T., Wallin, H., et al., 2017. Multi-walled carbon nanotube-physicochemical properties predict the systemic acute phase response following pulmonary exposure in mice. PLoS One 12, e0174167. https://doi.org/10.1371/journal.pone.0174167.
Rada, B., Park, J.J., Sil, P., Geiszt, M., Leto, T.L., 2014. NLRP3 inflammasome activation and interleukin-1β release in macrophages require calcium but are independent of calcium-activated NADPH oxidases. Inflamm. Res. 63, 821–830. https://doi.org/10.1007/s00011-014-0756-y.
Reimand, J., Kull, M., Peterson, H., Hansen, J., Vilo, J., 2007. g:Profiler–a web-based toolset for functional profiling of gene lists from large-scale experiments. Nucleic Acids Res. 35, W193–W200. https://doi.org/10.1093/nar/gkm226.
Ritchie, M.E., Phipson, B., Wu, D., Hu, Y., Law, C.W., Shi, W., et al., 2015. Limma powers differential expression analyses for RNA-sequencing and microarray studies. Nucleic Acids Res. 43, e47. https://doi.org/10.1093/nar/gkv007.
Rosas, I.O., Richards, T.J., Konishi, K., Zhang, Y., Gibson, K., Lokshin, A.E., et al., 2008. MMP1 and MMP7 as potential peripheral blood biomarkers in idiopathic pulmonary fibrosis. PLoS Med. 5, e93 https://doi.org/10.1371/journal.pmed.0050093.
Russell, W.M.S., Burch, R.L., 1959. The Principles of Humane Experimental Technique.
Russo, R.C., Garcia, C.C., Teixeira, M.M., Amaral, F.A., 2014. The CXCL8/IL-8 chemokine family and its receptors in inflammatory diseases. Expert. Rev. Clin. Immunol. 10, 593–619. https://doi.org/10.1586/1744666X.2014.894886.
Ryan, A.J., Larson-Casey, J.L., He, C., Murthy, S., Carter, A.B., 2014. Asbestos-induced disruption of calcium homeostasis induces endoplasmic reticulum stress in macrophages. J. Biol. Chem. 289, 33391–33403. https://doi.org/10.1074/jbc.M114.579870.
Rydman, E.M., Ilves, M., Koivisto, A.J., Kinaret, P.A.S., Fortino, V., Savinko, T.S., et al., 2014. Inhalation of rod-like carbon nanotubes causes unconventional allergic airway inflammation. Part Fibre Toxicol. 11, 48. https://doi.org/10.1186/s12989-014-0048-2.
Rydman, E.M., Ilves, M., Vanhala, E., Vippola, M., Lehto, M., Kinaret, P.A.S., et al., 2015. A single aspiration of rod-like carbon nanotubes induces asbestos-like pulmonary inflammation mediated in part by the IL-1 receptor. Toxicol. Sci. 147, 140–155. https://doi.org/10.1093/toxsci/kfv112.
Scala, G., Kinaret, P., Marwah, V., Sund, J., Fortino, V., Greco, D., 2018a. Multi-omics analysis of ten carbon nanomaterials effects highlights cell type specific patterns of molecular regulation and adaptation. NanoImpact. 11, 99–108. https://doi.org/10.1016/j.impact.2018.05.003.
Scala, G., Marwah, V., Kinaret, P., Sund, J., Fortino, V., Greco, D., 2018b. Integration of genome-wide mRNA and miRNA expression, and DNA methylation data of three cell lines exposed to ten carbon nanomaterials. Data Brief. 19, 1046–1057. https://doi.org/10.1016/j.dib.2018.05.107.
Scala, G., Serra, A., Marwah, V.S., Saarimäki, L.A., Greco, D., 2019. FunMappOne: a tool to hierarchically organize and visually navigate functional gene annotations in multiple experiments. BMC Bioinformatics. 20, 79. https://doi.org/10.1186/s12859-019-2639-2.
Serra, A., Fratello, M., del Giudice, G., Saarimäki, L.A., Paci, M., Federico, A., et al., 2020. TinderMIX: Time-dose integrated modelling of toxicogenomics data. Gigascience 9. https://doi.org/10.1093/gigascience/giaa055.
Sierra, M.I., Rubio, L., Bayón, G.F., Cobo, I., Menendez, P., Morales, P., et al., 2017. DNA methylation changes in human lung epithelia cells exposed to multi-walled carbon nanotubes. Nanotoxicology. 11, 857–870. https://doi.org/10.1080/17435390.2017.1371350.
Søs Poulsen, S., Jacobsen, N.R., Labib, S., Wu, D., Husain, M., Williams, A., et al., 2013. Transcriptomic analysis reveals novel mechanistic insight into murine biological responses to multi-walled carbon nanotubes in lungs and cultured lung epithelial cells. PLoS One 8, e80452. https://doi.org/10.1371/journal.pone.0080452.
Srivastava, R.K., Pant, A.B., Kashyap, M.P., Kumar, V., Lohani, M., Jonas, L., et al., 2011. Multi-walled carbon nanotubes induce oxidative stress and apoptosis in human lung

cancer cell line-A549. Nanotoxicology. 5, 195–207. https://doi.org/10.3109/17435390.2010.503944.

Stapleton, P.A., Hathaway, Q.A., Nichols, C.E., Abukabda, A.B., Pinti, M.V., Shepherd, D. L., et al., 2018. Maternal engineered nanomaterial inhalation during gestation alters the fetal transcriptome. Part Fibre Toxicol. 15, 3. https://doi.org/10.1186/s12989-017-0239-8.

Stoccoro, A., Di Bucchianico, S., Coppedè, F., Ponti, J., Uboldi, C., Blosi, M., et al., 2017. Multiple endpoints to evaluate pristine and remediated titanium dioxide nanoparticles genotoxicity in lung epithelial A549 cells. Toxicol. Lett. 276, 48–61. https://doi.org/10.1016/j.toxlet.2017.05.016.

Sun, B., Wang, X., Ji, Z., Wang, M., Liao, Y.-P., Chang, C.H., et al., 2015. NADPH oxidase-dependent NLRP3 inflammasome activation and its important role in lung fibrosis by multiwalled carbon nanotubes. Small 11, 2087–2097. https://doi.org/10.1002/smll.201402859.

Sun, S.-C., 2017. The non-canonical NF-κB pathway in immunity and inflammation. Nat. Rev. Immunol. 17, 545–558. https://doi.org/10.1038/nri.2017.52.

Vlasova, I.I., Kapralov, A.A., Michael, Z.P., Burkert, S.C., Shurin, M.R., Star, A., et al., 2016. Enzymatic oxidative biodegradation of nanoparticles: mechanisms, significance and applications. Toxicol. Appl. Pharmacol. 299, 58–69. https://doi.org/10.1016/j.taap.2016.01.002.

Wang, L., Luanpitpong, S., Castranova, V., Tse, W., Lu, Y., Pongrakhananon, V., et al., 2011. Carbon nanotubes induce malignant transformation and tumorigenesis of human lung epithelial cells. Nano Lett. 11, 2796–2803. https://doi.org/10.1021/nl2011214.

Webster, A.F., Chepelev, N., Gagné, R., Kuo, B., Recio, L., Williams, A., et al., 2015. Impact of genomics platform and statistical filtering on transcriptional benchmark doses (BMD) and multiple approaches for selection of chemical point of departure (pod). PLoS One 10, e0136764. https://doi.org/10.1371/journal.pone.0136764.

Yang, L., Allen, B.C., Thomas, R.S., 2007. BMDExpress: a software tool for the benchmark dose analyses of genomic data. BMC Genomics 8, 387. https://doi.org/10.1186/1471-2164-8-387.

Yu, J., Loh, X.J., Luo, Y., Ge, S., Fan, X., Ruan, J., 2020. Insights into the epigenetic effects of nanomaterials on cells. Biomater. Sci. 8, 763–775. https://doi.org/10.1039/c9bm01526d.

Zumerle, S., Calì, B., Munari, F., Angioni, R., Di Virgilio, F., Molon, B., et al., 2019. Intercellular calcium signaling induced by ATP potentiates macrophage phagocytosis. Cell Rep. 27 https://doi.org/10.1016/j.celrep.2019.03.011, 1–10.e4.